^{17}O NMR as a conclusive probe of charge-ordering models in half-doped manganites

A. Trokiner,[1] A. Yakubovskii,[1,2] S. Verkhovskii,[1,3] A. Gerashenko,[3] and D. Khomskii[4]
[1]*Laboratoire de Physique du Solide, E.S.P.C.I., UPR C.N.R.S. A05, Paris, France*
[2]*Russian Research Centre "Kurchatov Institute," Moscow, Russia*
[3]*Institute of Metal Physics, Ural Branch of Russian Academy of Sciences, Ekaterinburg, Russia*
[4]*II Physikalisches Institut, Universitaet zu Koln, Germany*
(Received 30 March 2006; published 20 September 2006)

We present a ^{17}O NMR study of the half-doped manganite, $Pr_{0.5}Ca_{0.5}MnO_3$ at $T \leqslant 10$ K. The charge-ordered and the ferromagnetic states are studied at $H=0$ and $H=12$ *T*, respectively. Since the ^{17}O nucleus probes spin and orbital configuration of its two first Mn neighbors, local magnetic environments of oxygen in different structural sites could be analyzed in both states. Local fields expected in two models of the charge-ordered state, the site-centered and the bond-centered ones, are compared to the experimental data. It is shown that the hierarchy of local fields at different oxygen sites favors the site-centered charge ordering with two different Mn sites.

DOI: 10.1103/PhysRevB.74.092403 PACS number(s): 75.30.Et, 75.47.Lx, 76.60.Cq, 76.60.Jx

Charge-ordering (CO) phenomena in perovskite manganites have been extensively studied due to an intriguing interplay of the charge, orbital, and spin degrees of freedom of these strongly correlated electron materials. The fine balance between the kinetic energy and the Coulomb interaction of electrons in the partially filled, high-spin, $3d$(Mn)-$2sp$(O) band results at low temperature in several possible ground states, mainly the ferromagnetic (FM) metallic and the CO insulating states, which can be altered by small changes in the chemical composition and under an applied magnetic field. The CO state is accompanied by an orbital ordering (OO). It is particularly pronounced in half-doped compounds, where the number of doped holes per Mn ion is a rational fraction—one per two Mn's.

Two alternative microscopic models of CO/OO were considered in the literature. The first model is the pure-ionic Mn^{3+}/Mn^{4+} model, originally proposed for $La_{0.5}Ca_{0.5}MnO_3$.[1] It involves the localization of an electron on Mn e_g orbital. The *ab*-plane pattern of Mn^{3+} and Mn^{4+} ions may be represented as a checkerboard of the corresponding $t_{2g}^3 e_g^1$ and t_{2g}^3 electronic configurations of Mn as shown in Fig. 1(a). The lobes of occupied e_g orbitals are directed as shown in this figure, giving FM double-exchange (DE) coupling[2,3] along corresponding bonds, whereas the antiferromagnetic (AF) superexchange t_{2g}-t_{2g} coupling dominates the magnetic interaction of Mn^{4+} and Mn^{3+} ions where the e_g lobes are perpendicular to the Mn^{3+}-O-Mn^{4+} bond.

Below T_N the competition of these exchange couplings results in the AF spin ordering of charge exchange (CE) type.[4] The ideal CE-type charge and orbital order implies a FM zigzag arrangement of the ordered $e_g(3x^2-r^2)$ and $e_g(3y^2-r^2)$ orbitals of Mn^{3+} ions in *ab* plane. The neighboring zigzags are AF coupled; the ordering in the *c* direction is also AF. The pure ionic picture with $3d^3/3d^4$ configurations should not be taken too literally. In fact, it is predicted theoretically that only a partial CO of the type $Mn^{3.5\pm\delta}$ should exist, with $\delta \sim 0.1/0.2$,[5,6] although the quantum numbers of corresponding states coincide with those of Mn^{4+} and Mn^{3+}. This model with two different Mn sites is also called site-centered model.

The alternative model of CO/OO is the bond-centered model which involves the trapping of an electron at some of the Mn-O-Mn bridges. It leads to the formation of the Zener-polaron state in the *ab* plane[7] as shown in Fig. 1(b). Inside

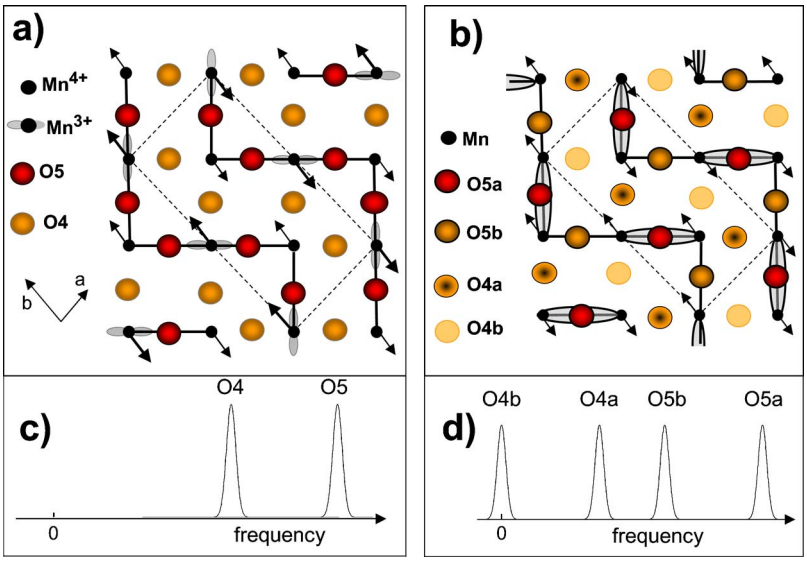

FIG. 1. (Color online) CE-type magnetic structure in the (a) site-centered and in the (b) Zener polaron CO/OO models. The ferromagnetic zigzags are indicated by the solid lines, and the dotted rectangle indicates the low temperature unit cell; only the *ab* plane is considered. The arrows show the Mn spins orientations. Schematic zero-field NMR spectrum expected for (c) the site-centered model—the two lines correspond to the local field experienced by the oxygen O5 and O4, inside and between the zigzags, respectively; (d) the Zener polaron model—the four lines correspond to the local field experienced by O5a, O5b, and O4a, O4b, inside and between the zigzags, respectively.

the dimer the Mn spins are FM correlated through DE, so that both Mn sites are equivalent and the average valence is +3.5. The dimers were treated in[7] as forming the same zigzags, while neighboring zigzags are AF coupled. The question of which picture of CO is indeed true is a hotly debated topic, both theoretically[8–10] and experimentally.[7,11–14]

Spatial ordering of electrons at given Mn orbitals or at (Mn-O-Mn) orbitals is accompanied by cooperative Jahn-Teller distortions in the MnO_6-octahedra sublattice. In the ionic model two Mn sites should exist, one of them $Mn^{3+}(3d^4)$, being far more distorted. Consequently many studies were devoted to the structural refinement of the CO phase, focusing mainly on the nonequivalent Mn ions in the cell and on the charge difference between two possible Mn configurations. It should be noted that it is rather difficult to distinguish from a structural point of view between these two models by x-ray or neutron powder-diffraction methods, due to incommensurability effects on the diffraction pattern.[12] Furthermore, it was reported that the long-range OO structure becomes commensurate only at a temperature far below T_{CO}.[11,15] For single crystals the main obstacle is the multidomain character of the CO/OO phase. Experimental x-ray studies,[13,14] electron microscopy[16] and neutron diffraction[11,13,15] support the site-centered model. It was found that the charge difference between the two Mn configurations is ~ 0.25,[13] ~ 0.16,[17] or ~ 0.15,[18] far from one unit charge expected for $3d^3/3d^4$ configurations but in agreement with theoretical calculations.[5,6] In fact, these calculations did not "support" the site-centered model, but rather assumed it, or at least assumed lattice symmetry which then produced the site-centered state. Other calculations[9,10] are rather in favor of a bond-centered state.

In manganites not many NMR studies were devoted to the CO state, and among them only two probe the ^{17}O nuclei.[19,20] Two interactions are expected for ^{17}O, the electric quadrupole interaction and the magnetic hyperfine interaction. In $Pr_{0.5}Ca_{0.5}MnO_3$ the first is far smaller than the latter interaction,[19] so that it is difficult to directly study charge disproportionation of Mn ions. Instead, ^{17}O nuclear spin is sensitive to its neighboring Mn spins and orbitals. Indeed, being placed between two Mn ions each ^{17}O nucleus probes the spin and orbital configuration of the corresponding Mn pair through the transferred spin density. In the charge disordered paramagnetic (CDPM) state or in a FM state all Mn ions are equivalent and only one ^{17}O NMR line exists. In the CO/OO phase, the splitting of the ^{17}O spectrum into several lines reflects the different local magnetic environments of the various O sites in the CE structure.

$Pr_{0.5}Ca_{0.5}MnO_3$ is one of the best systems to investigate the CO state since the onset of the CO ($T_{CO}=240$ K) and spin ($T_N=170$ K) orders are well separated in T.

In this Brief Report we present a NMR study at low temperature of the CO phase in $Pr_{0.5}Ca_{0.5}MnO_3$ probed by ^{17}O nuclei. We analyze local magnetic environment of oxygen at different structural sites within two microscopic models, the site-centered and the bond-centered model. The comparison of the predicted lines with the ^{17}O NMR spectra obtained at $T<10$ K unambiguously shows that the CO phase of $Pr_{0.5}Ca_{0.5}MnO_3$ is in agreement with the site-centered CO model with two different Mn sites.

We used a $Pr_{0.5}Ca_{0.5}MnO_3$ sample prepared as a powder with an average grain size ~ 2 μm using a "paper synthesis" described in Ref. 21. With this method, the accuracy of the cationic ratio Pr/Ca=0.5/0.5 is better than 1.00(5) within each grain. The powder was enriched with ^{17}O isotope up to $\approx 25\%$, and the single-phase nature of the enriched sample was confirmed by x-ray diffraction at room temperature. The onset of the CO order was found to occur at $T_{CO}=240(5)$ K Probably due to the small grain size of our sample, the melting of the CO into the FM state occurs at a reduced field compared to single crystals[22] giving us the advantage to investigate both the FM and CO phase by NMR at 11.7 T.

Spectra were obtained in zero-field NMR and at $H_0=11.7$ T with point-by-point frequency sweep. The intensity of the spin-echo signal formed after the pulse sequence $(\pi/2)-t_{del}-(\pi)$-echo was measured at each frequency point. The width of the $\pi/2$ pulse was 1.2 μs and t_{del}, the delay varied in the range (15–200) μs. The intensities were corrected to $t_{del}\approx 0$ by measuring the echo-decay rate at different frequencies of the spectrum. The quality factor Q of the NMR coil, the impedance of the resonant circuit and the gain of the power amplifier were controlled at every point of the wide spectrum. Such a care is required to obtain in the whole frequency range an echo-signal voltage, $V(t=0,\nu)$, only proportional to the intensity $^{17}\mathrm{Int}(\nu)$ multiplied by ν^2. Thus, the fraction of oxygen contributing to an echo at a given frequency is directly obtained.

The local magnetic field at O sites $^{17}h_{loc}$ originates from the Fermi-contact interaction with the transferred s-spin density of electrons participating in the Mn-O-Mn bonding. Considering one first Mn neighbor $^{17}h_{loc}$ is

$$^{17}\boldsymbol{h}_{loc}=H_{FC}(2s)f_s\boldsymbol{\mu}_{eff}(\mathrm{Mn})/\mu_B. \quad (1)$$

Here, μ_{eff}(Mn) is the effective magnetic moment of the Mn ion. $H_{FC}(2s)=1.1$ MOe (Ref. 23) is the corresponding hyperfine magnetic field due to the Fermi-contact interaction with one unpaired electron located on the $2s$ orbital. Following[24] the corresponding isotropic spin density transferred to oxygen from the neighboring Mn ion is defined in terms of the factor $f_s=h_{loc}/H(2s)$ for $\mu_{eff}=1\mu_B$. The sign and magnitude of the transferred s-wave spin polarization is due to the covalent mixing of the $2s$(O) orbital with the partially filled/empty e_g(Mn) orbital.[24] The corresponding overlap integral, defined by the scalar product $S_s=\langle 2s(\mathrm{O})|e_g(\mathrm{Mn})\rangle$, depends to a much smaller extent ($|\Delta S_s/S_s|\leqslant 0.1$) on the variance of the Mn-O-Mn bond bending or/and the interatomic distance, $d_{\mathrm{Mn\text{-}O}}=(1.90-2.06)$ Å[11] occurring in the CO phase of $Pr_{0.5}Ca_{0.5}MnO_3$. The peculiar covalent mixing effects make ^{17}O NMR a sensitive tool in respect to the particular spin and orbital configuration of the neighboring Mn.

At $T=10$ K and $H_0=12$ T both the CO AF and FM metallic phases coexist in our sample. At low T the Mn spin dynamic in the FM-ordered domains becomes extremely slow compared to the rather moderate one in the CO regions with still nonmelted AF spin order. We have the following relations for the nuclear spin lattice, $^{17}T_1$, and the spin-spin $^{17}T_2$ relaxation times of ^{17}O in $Pr_{0.5}Ca_{0.5}MnO_3$ in both

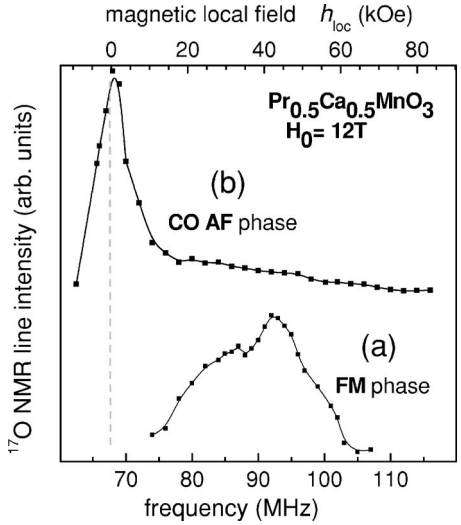

FIG. 2. ^{17}O NMR spectra in $Pr_{0.5}Ca_{0.5}MnO_3$ measured at $T=10$ K and $H_0=12$ T. (a) FM phase of the field-cooled sample: $t_{del}=160$ μs, $t_{rep}=2$ s; (b) CO AF phase of the zero-field-cooled sample: $t_{del}=15$ μs, $t_{rep}=100$ ms.

phases, $^{17}T_1(\mathrm{FM})>1\ \mathrm{s}\gg{}^{17}T_1(\mathrm{AF})\sim 0.1$ s and $^{17}T_2(\mathrm{FM})\sim 500\ \mu\mathrm{s}\gg{}^{17}T_2(\mathrm{AF})$, with $^{17}T_2(\mathrm{AF})\leqslant 100\ \mu$s. By adjusting the repetition time t_{rep} and t_{del}, we can obtain selectively the spectrum from FM and CO AF domains.

The ^{17}O NMR spectrum due to the FM domains [Fig. 2(a)] consists of a single broad line shifted to the higher frequency, $\Delta\nu(O_{FM})=25.0(5)$ MHz, with respect to the Larmor frequency, $\nu_L=67.8$ MHz of ^{17}O in H_2O. The shift corresponds to $^{17}h_{loc,FM}=43(2)$ kOe created by s-wave spin density transferred from two neighboring $Mn^{+3.5}$ ions. Taking in Eq. (1) $\mu_{eff}(Mn^{+3.5})=3.5\mu_B$ in the saturated FM state of $Pr_{0.5}Ca_{0.5}MnO_3$,[22] we obtain the factor $f_{s,FM}=0.0055(5)$, very close to the corresponding value in the CDPM phase, $f_{s,CDPM}=0.0050(5)$.[19]

The ^{17}O NMR spectrum shown in Fig. 2(b) originates from CO AF domains. It was performed at $T=10$ K and $H=12$ T after zero field cooling the sample. Its intensity was optimized using a fast repetition time ~50 ms. The spectrum splits into two parts. The narrow line near ν_L originates from oxygen with a vanishing $^{17}h_{loc}$. As shown in Refs. 19 and 20, the local field is greatly reduced at the oxygen sites between ab planes (apical oxygen), since both neighboring Mn ions from adjacent ab planes are in the same valence state and their spins are AF correlated. In the Zener polaron scenario,[7] $^{17}h_{loc}$ should also cancel at the oxygen located between the AF-correlated adjacent dimers of $Mn^{3.5+}$ (O4b sites) as shown in Fig. 2(b). The broad part of the CO AF spectrum is due to oxygen sites in the ab plane with a nonzero $^{17}h_{loc}$. However, due to the angle averaging effect in a powder, the spectrum is not resolved. One possible origin is the canting of the AF-ordered Mn spins at 12 T. Indeed, the local field at Mn sites being $^{55}h_{loc,on\text{-}site}(\mathrm{Mn})>30$ T,[25] the canting contributes mainly to the broadening of the spectrum.

The ^{17}O NMR spectrum shown in Fig. 3 was measured at 4.2 K in zero external field (ZF NMR). In these conditions only the CO AF phase exists in $Pr_{0.5}Ca_{0.5}MnO_3$. Compared

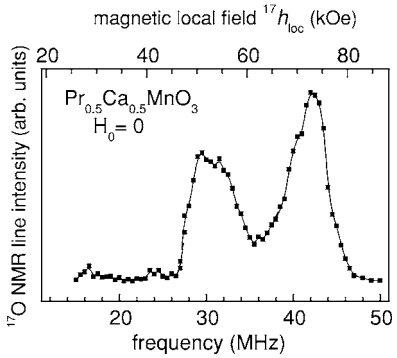

FIG. 3. ^{17}O zero field NMR spectrum measured at $T=4.2$ K in $Pr_{0.5}Ca_{0.5}MnO_3$ (CO AF phase).

to NMR, the ZF NMR powder spectrum is far better resolved; its resolution is comparable to that of an untwinned single crystal. As compared to incomplete ZF NMR spectrum presented in Ref. 20, the spectrum at Fig. 3 of the present paper is substantially extended to the low-frequency side, thus covering all the NMR lines contributed by oxygen with different magnetic environment in the ab plane. In the explored frequency range $\nu=(15-50)$ MHz, there are only two lines; no line is detected between 15 and 28 MHz. These two lines are peaked at 31(1) MHz ($^{17}h_{loc}=54(2)$ kOe and 41(1) MHz ($^{17}h_{loc}=71(2)$ kOe, with a relative intensity 0.46(4) and 0.54(4), respectively. As $^{17}h_{loc}$ is nonzero, both lines originate from O sites in the ab plane.

Let us discuss the ZF NMR spectrum in the framework of two competing microscopic descriptions of CO/OO in $Pr_{0.5}Ca_{0.5}MnO_3$. For the site-centered model, the schematic expected ZF NMR spectrum [Eqs. (2a) and (2b)] is shown in Fig. 1(c). It consists of two lines corresponding to $^{17}h_{loc}$ experienced by the oxygen O5 and O4, inside and between the zigzags, respectively. In the experimental spectrum at Fig. 3 the high- and low-frequency peaks are attributed to oxygen in the O5 and the O4 sites, respectively. Indeed, for the O5 site the transferred spin density is the largest, since within a zigzag the lobe of the e_g-orbital of Mn^{3+} ions points toward the neighboring oxygen. Furthermore, the two neighboring Mn ions of O5 are FM correlated. In terms of transferred s-wave polarization the following expression can be suggested for $^{17}h_{loc}$ at the O5 site due to its two Mn neighbors:

$$^{17}\boldsymbol{h}_{loc}(\mathrm{O5})\mu_B = H_{FC}(2s)\{f_{s,3}\boldsymbol{\mu}_{eff}(\mathrm{Mn}^{3+}) + f_{s,4}\boldsymbol{\mu}_{eff}(\mathrm{Mn}^{4+})\}. \quad (2a)$$

For O4 we expect a nonzero local field $^{17}h_{loc}$(O4) for the following reasons. Although the spins of Mn in adjacent zigzags are antiparallel, the O4 oxygen is "sandwiched" between Mn^{3+} and Mn^{4+} ions with different spin values and orbital occupations. This results in a substantial local field, although smaller than for O5. Moreover, the transferred s-wave polarization from the Mn^{4+} ion is expected to be negative due to effects of covalent mixing with the empty e_g orbitals.[24] Thus, $^{17}h_{loc}$(O4) can be expressed through the s-wave transferred spin density $f_{s,3}\mu(\mathrm{Mn}^{3+})$ and $f_{s,4}\mu(\mathrm{Mn}^{4+})$ of the two neighboring Mn with $f_{s,3}>0$ and $f_{s,4}<0$ as

$$^{17}\boldsymbol{h}_{loc}(\mathrm{O4})\mu_B = H_{FC}(2s)\{0.25 f_{s,3}\boldsymbol{\mu}_{eff}(\mathrm{Mn}^{3+}) - f_{s,4}\boldsymbol{\mu}_{eff}(\mathrm{Mn}^{4+})\}. \quad (2b)$$

The sign "+"/"−" in (2a) and (2b) takes into account the FM/AF spin order of the Mn^{3+} and Mn^{4+} neighboring ions; the factor 0.25 means that for O4 the large Mn^{3+} e_g lobe is orthogonal to the Mn-O bond, in contrast to the O5 case. It is worth noting the significant difference in the spin-density transfer factors $f_{s,3}=0.022$ and $|f_{s,4}|=0.009$ deduced from Eqs. (2a) and (2b), and Fig. 3. Such a large value of the $f_{s,3}$ factor indicates a substantial delocalization of the e_g hole within the hybridized $e_g(\mathrm{Mn}^{3+})$-$2p\sigma(\mathrm{O})-2s(\mathrm{O})$ orbital.[6]

The bond-centered model of Fig. 1(b) predicts four magnetically different O sites with local fields, expressed as,

$$^{17}\boldsymbol{h}_{loc}(\mathrm{O5}a)\mu_B = H_{FC}(2s)\{2 f_{s,3.5}\boldsymbol{\mu}_{eff}(\mathrm{Mn}^{3.5+})\}, \quad (3a)$$

$$^{17}\boldsymbol{h}_{loc}(\mathrm{O5}b)\mu_B = H_{FC}(2s)\{f_{s,3.5}\boldsymbol{\mu}_{eff}(\mathrm{Mn}^{3.5+}) + 0.25 f_{s,3.5}\boldsymbol{\mu}_{eff}(\mathrm{Mn}^{3.5+})\}, \quad (3b)$$

$$^{17}\boldsymbol{h}_{loc}(\mathrm{O4}a)\mu_B = H_{FC}(2s)\{f_{s,3.5}\boldsymbol{\mu}_{eff}(\mathrm{Mn}^{3.5+}) - 0.25 f_{s,3.5}\boldsymbol{\mu}_{eff}(\mathrm{Mn}^{3.5})\}, \quad (3c)$$

$$^{17}\boldsymbol{h}_{loc}(\mathrm{O4}c)\mu_B = 0. \quad (3d)$$

The predicted ZF NMR spectrum is sketched in Fig. 1(d). It consists of four lines of equal intensity peaked at the frequencies $\nu_i=(^{17}\gamma/2\pi)^{17}h_{loc,i}$ which are ordered as follows: $\nu(\mathrm{O5}a), \nu(\mathrm{O5}b)=0.612\nu(\mathrm{O5}a), \nu(\mathrm{O4}a)=0.375\nu(\mathrm{O5}a)$, and $\nu(\mathrm{O4}b)=0$. Taking into account the number, as well as the position of the peaks, the predicted spectrum is not consistent with the experimental one (Fig. 3). Moreover, in the bond-centered model due to the DE mechanism the coupling between Mn spins inside a polaron is definitely strongly ferromagnetic. Thus, according to Eq. 3(a) the O5a oxygen experiences the largest local field, $^{17}h_{loc}(\mathrm{O5}a)$ and this field should be the same as in the saturated FM state. As in the FM state, the peak position is $\Delta\nu(\mathrm{O}_{FM})=25.0(5)$ MHz [Fig. 2(a)], in the AF CO phase the O5a line should peak at the same frequency but as shown in Fig. 3, it peaks at 41 MHz. Again, the prediction of the bond-centered model is not consistent with the comparison of the CO AF and FM states results.

Summarizing, we have shown that ^{17}O NMR provides a direct probe of the Mn spin and orbital correlations in the charge-ordered phase of manganites. The analysis of the number of ^{17}O NMR lines and of the corresponding local fields $^{17}h_{loc}$ in the charge-ordered antiferromagnetic, as well as in the ferromagnetic metallic phases, unambiguously shows that for half-doped $Pr_{0.5}Ca_{0.5}MnO_3$ the site-centered checkerboard CE structure is realized, and not that of bond-centered Zener polarons. We have explored in Ref. 20 an opportunity of using the ^{17}O NMR in the external field as a tool for the check-in of the CO in half-doped bismuth manganites. Our conclusion, that ^{17}O NMR data analysis favors the bond-centered model of CO in these manganites, is not altered. Evidently, the line counting in zero-field spectrum of CO AF phase is a more conclusive way as compared to an analysis of the NMR spectrum, measured in an external field and presenting substantially smaller resolution. Unfortunately, zero-field spectra shown in Fig. 3 (Ref. 20) were not completed at the low-frequency side. The question, whether bond-centered ordering, or a combination of both, can exist at other doping levels, deserves further study; it can be also addressed by using oxygen NMR.

The authors thank N. Bontemps for useful discussions. This work is supported in part by the Russian Foundation for Basic Research (Grants No. 05-02-16645, No. 06-02-17386, and No. 06-02-91171). S.V. and A.Y. are grateful to ESPCI for hospitality and support.

[1] J. Goodenough, Phys. Rev. **100**, 564 (1955).
[2] C. Zener, Phys. Rev. **82**, 403 (1951).
[3] P.-G. de Gennes, Phys. Rev. **118**, 141 (1960).
[4] E. O. Wollan and W. C. Koehler, Phys. Rev. **100**, 545 (1955).
[5] J. van der Brink, G. Khaliullin, and D. Khomskii, Phys. Rev. Lett. **83**, 5118 (1999).
[6] V. Anisimov, I. S. Elfimov, M. A. Korotin, and K. Terakura, Phys. Rev. B **55**, 15494 (1997).
[7] A. Daoud-Aladine, J. Rodríguez-Carvajal, L. Pinsard-Gaudart, M. T. Fernández-Diaz, and A. Revcolevschi, Phys. Rev. Lett. **89**, 097205 (2002).
[8] D. Efremov, J. van den Brink, and D. Khomskii, Nat. Mater. **3**, 853 (2004).
[9] G. Zheng and C. H. Patterson, Phys. Rev. B **67**, 220404(R) (2003).
[10] V. Ferrari, M. Towler, and P. B. Littlewood, Phys. Rev. Lett. **91**, 227202 (2003).
[11] Z. Jirak, F. Damay, M. Hervieu, C. Martin, B. Raveau, G. Andre, and F. Bouree, Phys. Rev. B **61**, 1181 (2000).
[12] P. G. Radaelli, D. E. Cox, M. Marezio, and S-W. Cheong, Phys. Rev. B **55**, 3015 (1997).
[13] R. J. Goff and J. P. Attfield, Phys. Rev. B **70**, 140404(R) (2004).
[14] S. Grenier *et al.*, Phys. Rev. B **69**, 134419 (2004).
[15] R. Kajimoto, H. Yoshizawa, Y. Tomioka, and Y. Tokura, Phys. Rev. B **63**, 212407 (2001).
[16] S. Mori, T. Katsufuji, N. Yamamoto, C. H. Chen, and S-W. Cheong, Phys. Rev. B **59**, 13573 (1999).
[17] J. Herrero-Martín, J. García, G. Subías, J. Blasco, and M. Concepción Sánchez, Phys. Rev. B **70**, 024408 (2004).
[18] K. Thomas *et al.*, Phys. Rev. Lett. **92**, 237204 (2004).
[19] A. Yakubovskii, A. Trokiner, S. Verkhovskii, A. Gerashenko, and D. Khomski, Phys. Rev. B **67**, 064414 (2003).
[20] A. Trokiner *et al.*, Phys. Rev. B **72**, 054442 (2005).
[21] A. M. Balagurov, V. Yu. Pomjakushin, D. V. Sheptyakov, V. L. Aksenov, P. Fischer, L. Keller, O. Yu. Gorbenko, A. R. Kaul, and N. A. Babushkina, Phys. Rev. B **64**, 024420 (2001).
[22] M. Tokunaga, N. Miura, Y. Tomioka, and Y. Tokura, Phys. Rev. B **57**, 5259 (1998).
[23] S. Fraga, J. Karwowski, and K. Saxena, *Handbook of Atomic Data* (Elsevier Scientific, Amsterdam, 1976).
[24] R. Watson and A. Freeman, in *Hyperfine Interactions* (Academic Press, New York, 1967).
[25] G. Allodi, R. De Renzi, F. Licci, and M. W. Pieper, Phys. Rev. Lett. **81**, 4736 (1998).